Defect clustering in Fe- and Al-substituted $YBa_2Cu_3O_7$

M. S. Islam and C. Ananthamohan
Department of Chemistry, University of Surrey, Guildford, GU2 5XH United Kingdom
(Received 6 May 1991)

Atomistic simulation techniques are used to investigate the effect of Fe and Al dopant substitution in $YBa_2Cu_3O_7$. Interatomic potentials that were previously developed for the oxide are employed, which correctly reproduce the orthorhombic crystal structure. From the calculated defect energies, values of the binding energies are derived for various dopant-oxygen interstitial clusters on the Cu(1) basal plane. The cluster configurations considered range in size from the simple dimer, containing two dopant ions, to large clusters containing up to seven dopant ions. The results indicate a strong tendency towards cluster formation, rather than a random distribution of defect species. This leads to an increase in the Fe (or Al) site coordination with oxygen. Ion displacements following lattice relaxation about the dopants are also examined. We calculate significant off-center displacement of both Fe and Al ions and find a lengthening of the bond with the apex oxygen, O(4). Our results are in line with recent neutron-diffraction and x-ray-absorption studies that find evidence for defect clustering in doped samples.

I. INTRODUCTION

The effects of partial metal substitution on the superconducting and structural properties of the $YBa_2Cu_3O_7$ material have been extensively studied.[1–28] In particular, the relative importance of the two distinct copper sites, Cu(1) chain and Cu(2) plane, has been examined by introducing cation dopants that preferentially substitute for one of these two sites, to obtain an insight into the origin of its superconductivity.

X-ray- and neutron-diffraction, x-ray-absorption, and Mössbauer spectroscopy studies[3,4,15,20,23–27] generally find that Fe and Al substitute only or predominantly for the Cu(1) chain site. Such doping results in a depression of T_c, an orthorhombic to tetragonal phase transformation, and an increase in oxygen content. However, the relation between these different effects and the mechanism of T_c suppression is still uncertain.

For Fe substitution there are significant differences in the interpretation of the data obtained, particularly from ^{57}Fe Mössbauer measurements, with some studies suggesting the presence of both Fe^{3+} and Fe^{4+}. In addition, the precise nature of the local structure about Fe and Al substitutionals is not well characterized due to the various types of oxygen coordinations possible in the oxygen-variable Cu(1) layer. Indeed, it cannot be assumed that the local dopant configuration is the same as the configuration about a normal copper site.

It has become increasingly clear that the suppression of T_c may be closely related to perturbations in the local structure; this includes the possible association of dopants with their charge-compensating defects to form distinct clusters. In fact, a number of recent experimental studies[23–28] have found evidence for dopant clustering on the Cu(1) basal plane, revealing more complex aspects than earlier investigations.

The diffuse scattering from early electron-diffraction studies of Bordet *et al.*[23] was interpreted in terms of linear Fe clusters having a width of a few cations. Bridges *et al.*[25] analyzed their data from extended x-ray-absorption fine-structure (EXAFS) measurements in terms of "clumping" of dopant ions (Co^{3+} or Fe^{3+}) into zigzag type chains with some off-center displacement. From neutron diffraction and Mössbauer studies, Dunlap *et al.*[24] suggest short-chain Fe clusters with a slight displacement of the Fe substitutional off the Cu(1) site. Katsuyama *et al.*[28] have also reported diffraction and Mössbauer measurements and proposed the formation of Fe clusters such as dimers, trimers, or tetramers on the Cu(1) layer. More recently, x-ray-absorption near-edge spectroscopy (XANES) studies of Yang *et al.*[26,27] suggest the formation of Fe^{3+}—O—Fe^{3+} linkages on the linear chains due to incoming oxygen, although they found no evidence for zigzag configurations, in contrast with the results of Bridges *et al.*[25]

Clearly, these results further emphasize the need to examine defect structures on a local scale[29] in order to fully understand the relation between structural behavior and superconductivity. The importance of local structural changes is not surprising since the coherence length of the hole pairs is relatively short (approximately 10–50 Å) in the high-T_c cuprates. However, despite the numerous dopant studies little quantitative information on cluster structures and relative binding energies has emerged. This is partly due to inhomogeneity problems and the extreme sensitivity of oxygen stoichiometry to processing conditions, making any experimental analysis of local structure more difficult.

The aim of the present study is to use established atomistic computer simulation techniques to further elucidate the cluster structures of Fe^{3+}- and Al^{3+}- substituted $YBa_2Cu_3O_7$. Simulation methods have proved to be particularly useful in examining the stability of defects and defect clusters in a diverse range of polar solids, from nonstoichiometric binary oxides,[30,31] and Li-intercalated spinels[32] to fluorite-structured halides.[33] Consequently, a

number of studies using such techniques on high-T_c superconducting oxides have been reported. These include simulations of crystal structure, defect chemistry, and bipolaron phenomena in La_2CuO_4,[34–36] $YBa_2Cu_3O_7$,[37–39] and the bismuth cuprates.[40]

Our previous investigations of $YBa_2Cu_3O_7$ focused on oxygen migration mechanisms[39] and impurity substitution at high dilution.[38] The latter study predicted well the effects of doping with metal ions including preferential substitutional sites on the copper sublattice, and also found a trend between T_c and calculated Cu(1)—O(4) bond distances that is consistent with neutron diffraction data. Our concern in the present study is to extend previous work by attempting to understand how Fe^{3+} and Al^{3+} dopants on the Cu(1) layer might associate with their charge-compensating defects (i.e., oxygen interstitials). For this task the atomistic simulation methods are well suited as they model accurately the Coulomb and relaxation energies, which are the predominant terms in any localized clustering process.

II. SIMULATION METHODS

The crystal lattice simulations are based on energy minimization procedures and Mott-Littleton methodology embodied in the CASCADE (Ref. 41) and HADES (Ref. 42) suite of programs. Extensive discussions of these widely used techniques are given by Catlow.[43,44]

The calculations are formulated within the framework of the Born model, with the interatomic forces represented by effective pairwise potentials of the following form:

$$\phi_{ij}=\frac{Z_iZ_je^2}{r_{ij}}+A_{ij}\exp(-r_{ij}/\rho_{ij})-C_{ij}/r_{ij}^6 \ . \tag{1}$$

The first term is the long-range Coulombic interaction and is summed accurately by means of the Ewald method. The remaining terms correspond to short-range interactions, which are represented by an analytical function of the Buckingham form. It should be stressed, as argued previously,[45] that employing the Born model does not necessarily mean that the electron distribution corresponds to a fully ionic system, and that the general validity of the potential model is assessed principally by its ability to reproduce observed crystal properties.

Ionic polarization is treated by the shell model[46] which represents each ion in terms of a massless shell, simulating the polarizable valence electrons, connected by a harmonic spring to a core in which the mass of the ion is concentrated. The overall charge on the ion is partitioned between the core and the shell, so that the free-ion polarizability is given by $\alpha=Y^2/k$, where Y is the shell charge and k is the harmonic spring constant. Since short-range repulsions are taken to act between shells, the model includes the important coupling between the repulsive forces and polarization. Despite this simple mechanical representation of the ionic dipole, the shell model has been shown to correctly simulate both dielectric and elastic properties, and is essential for reliable calculations of defect energies.

In the present investigation the same interatomic potentials and shell-model parameters are used as in our previous modeling studies of $YBa_2Cu_3O_7$,[37–39] in which all the Cu ions are considered in the 2+ charge state. This favored potential model reproduced the observed crystal structure to within 0.03 Å and predicted oxygen vacancy and impurity substitution sites in agreement with experiment. Alternative distributions of charge were not as successful at either reproducing the orthorhombic structure or deriving stable potentials with respect to calculated phonon dispersion curves. Moreover, our assignment is consistent with photoemission experiments[47–50] which find no evidence for Cu^{3+} ground-state ions. Full details of the potential parameters and calculated crystal properties for $YBa_2Cu_3O_7$ are given by Baetzold.[37] With regard to the Fe- and Al-host interactions, the potentials are taken from studies of the corresponding binary oxides,[51] which were derived by empirical fitting to observed crystal properties.

A vital feature of the defect simulations is the treatment of lattice relaxation around the defect or impurity center. The effect is generally large because the charged defect provides an extensive perturbation of the surrounding lattice. The Mott-Littleton approach[52,53] is to divide the crystal into two regions, so that ions in the central inner region (I) immediately surrounding the defect are explicitly minimized using specified interatomic potentials, while the remainder of the crystal (region II) is treated as a polarizable dielectric continuum. The explicit simulation of region I uses efficient energy minimization methods which make use of first and second derivatives of the energy function with respect to ion coordinates.

The total energy of the defects in the crystal may be written formally as

$$E=E_1(\mathbf{x})+E_2(\mathbf{x},\mathbf{y})+E_3(\mathbf{y}) \ , \tag{2}$$

where E_1 is the energy of region I (whose ion positions are described by the coordinate vector $\mathbf{x}$); E_3 depends solely on the positions ($\mathbf{y}$) of ions within region II; E_2 represents the interaction between the two regions. In this way the simulations can calculate the formation energies of defect species (such as dopant substitutionals) as well as predict local ion displacements during lattice relaxation.

III. RESULTS AND DISCUSSION

A. Cluster configurations

For Fe^{3+} and Al^{3+} ions substituting at Cu^{2+} chain sites there are two alternative types of extrinsic defect that may be created to preserve charge neutrality: oxygen interstitials or copper vacancies. The corresponding defect reactions can be represented by the following:

$$M_2O_3+\text{crystal}=2M_{Cu}^{\cdot}+O_i''+2CuO \ , \tag{3}$$

$$M_2O_3+\text{crystal}=2M_{Cu}^{\cdot}+V_{Cu}''+3CuO \ , \tag{4}$$

indicating a ratio of two trivalent dopants to one charge-compensating defect. (In the Kroger-Vink notation,[54] which is used in this paper, vacancy, interstitial and sub-

stitutional defects are donated as V_{Cu}, O_i, and M_{Cu}, respectively.)

From our previous study[38] of isolated dopants, the process involving oxygen incorporation [Eq. (3)] was found to have the lowest energy and is predicted to be that most likely to occur. This is in agreement with thermogravimetric and neutron experiments[4,18,23] that show an increase in oxygen content with increasing Fe^{3+}, Al^{3+}, and Co^{3+} concentration.

Our earlier simulations treated impurities and oxygen interstitials as isolated noninteracting species and so referred to systems at high dilution. However, these species carry opposite virtual charges and, thus, likely to associate at high dopant concentrations. It is well established that interactions between aliovalent impurity ions and their charge-compensating defects can lead to the formation of distinct defect clusters, largely due to Coulombic forces.

Consequently, we have identified various two-dimensional cluster configurations comprised of nearest-neighbor Fe^{3+} (or Al^{3+}) substitutionals and oxygen interstitials on the Cu(1) basal plane. Note that within the orthorhombic structure of pure $YBa_2Cu_3O_7$ each Cu(1) chain site is adjacent to an unoccupied (or interstitial) position, O(5). It is, therefore, possible to visualize the substitution of chain Cu^{2+} ions by trivalent dopants leading to the incorporation of oxygen ions into these neighboring unoccupied *a* sites.

The simplest neutral cluster that may form is one containing two neighboring impurity ions and an oxygen ion at the interstitial position between them. This *M*—O—*M* linkage or dimer configuration is shown in Fig. 1. For the more complex neutral tetramer, consisting of four impurity ions and two oxygen interstitials, a number of

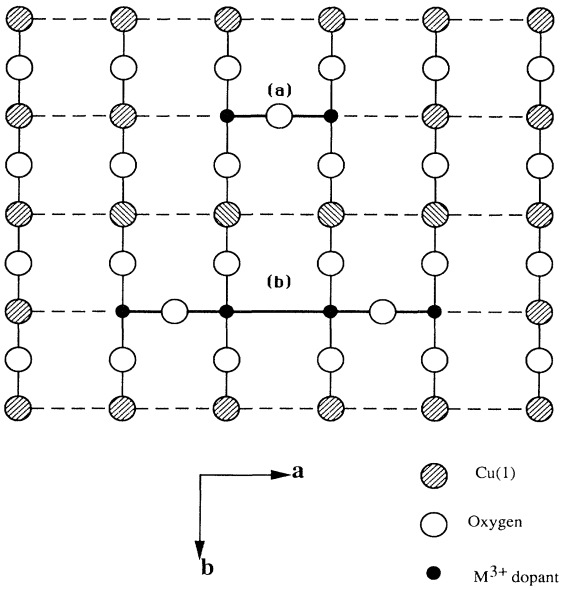

FIG. 1. Dopant substitutional-oxygen interstitial clusters in the Cu(1) layer (a) dimer; (b) collinear tetramer.

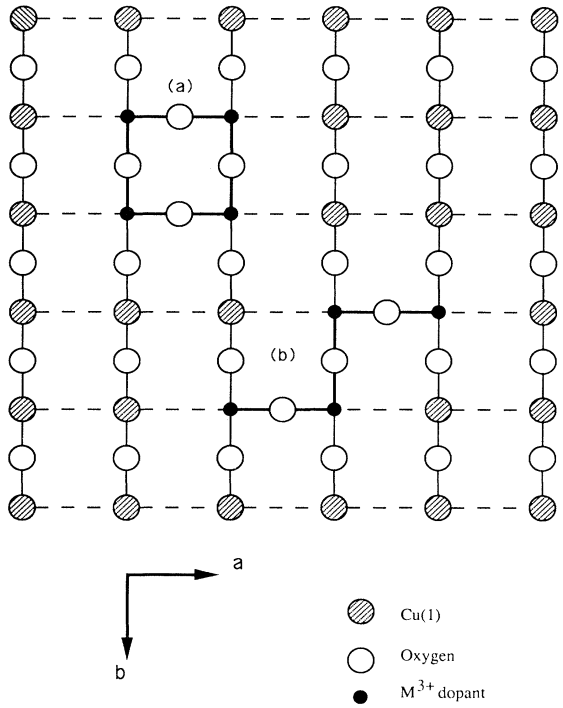

FIG. 2. Dopant substitutional-oxygen interstitial clusters in the Cu(1) layer (a) square tetramer; (b) zigzag tetramer.

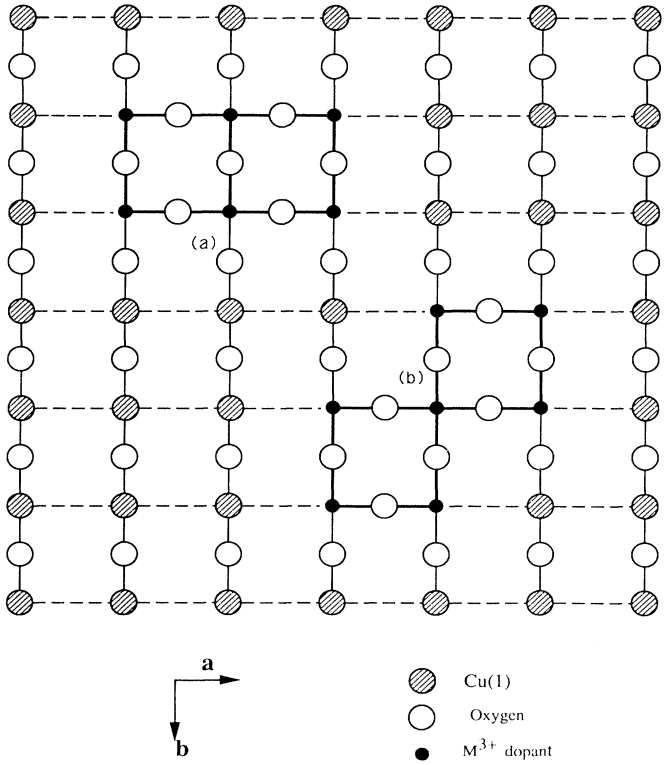

FIG. 3. Dopant substitutional-oxygen interstitial clusters in the Cu(1) layer (a) ($6M_{Cu}^{\cdot}$-$4O_i''$) hexamer; (b) ($7M_{Cu}^{\cdot}$-$4O_i''$) double chain.

different configurations may arise. Three possible geometries are identified: linear, square, and zigzag, which are illustrated in Figs. 1 and 2. Finally, we considered two large clusters shown in Fig. 3, which we refer to as hexamer and double-chain configurations. These two cluster types can be viewed in terms of edge sharing and corner sharing of the square tetramer unit.

B. Cluster stability (binding energies)

Due to the number of simple clusters that are possible and their microscopic nature an unambiguous interpretation of any structural data can be difficult. Therefore, reliable values for binding (or association) energetics from simulation methods, which are able to probe defect structures on a local scale, are particularly useful. The simulation approach is based on the calculation of cluster-binding energies with respect to the constituent defects, i.e., according to the following equation (in the case of the dimer configuration):

$$E_b = E(2M_{Cu}^{\cdot}O_i'') - 2E(M_{Cu}^{\cdot}) - E(O_i'') , \quad (5)$$

where the first term is the total energy of the cluster, and the remaining terms are the energies of an isolated substitutional and an isolated oxygen interstitial. The energy of an isolated oxygen interstitial is simply that required to introduce the O^{2-} ion to the site from infinity; while the value for the substitutional species includes both the energy required to remove the Cu^{2+} ion from the lattice and the energy to introduce the dopant (Fe^{3+} or Al^{3+}) ion to the site from infinity.

The calculated binding energies for the different clusters are reported in Tables I to IV. Because of the size of these clusters, the calculations were carried out using a larger inner region (I) containing 300 ions to ensure the defect energy closely approaches its limiting value. Our sign convention is such that a negative value for the binding energy indicates the system is bound. Also, to assist in the comparison of different configurations the binding energies are given per constituent dopant ion in the cluster. For example, for the dimer the energy reported is the total binding energy divided by two.

As well as dopant-oxygen clusters, calculations were first performed on clusters containing only nearest-neighbor dopant ions. The results in Tables I and II for Fe^{3+} and Al^{3+}, respectively, clearly show that such aggregates of two, three, or four dopant ions are unstable with respect to isolated ions. This indicates that this mode of aggregation would not give rise to defect clustering—a result that is not surprising in view of the effective repulsion between the cation species.

TABLE I. Energetics of clusters of nearest-neighbor Fe^{3+} substitutionals on the Cu(1) layer.

Cluster	Total defect energy (eV)	Binding energy[a] (eV/dopant)
$Fe_{Cu}^{\cdot}$	−18.26	—
$2Fe_{Cu}^{\cdot}$	−35.92	0.30
$3Fe_{Cu}^{\cdot}$	−53.35	0.48
$4Fe_{Cu}^{\cdot}$	−70.27	0.70

[a]Negative value indicates system is bound.

TABLE II. Energetics of clusters of nearest-neighbor Al^{3+} substitutionals on the Cu(1) layer.

Cluster	Total defect energy (eV)	Binding energy (eV/dopant)
$Al_{Cu}^{\cdot}$	−23.79	—
$2Al_{Cu}^{\cdot}$	−46.99	0.30
$3Al_{Cu}^{\cdot}$	−70.27	0.37
$4Al_{Cu}^{\cdot}$	−92.44	0.68

In Tables III and IV the calculated energetics of the Fe- and Al-oxygen interstitial clusters are presented. Examination of the results reveals that in both cases the clusters are found to be bound with large binding energies indicating a high degree of stability. This strongly suggests that there will be a greater tendency toward clustering and less random distribution at higher dopant concentrations, in agreement with experimental evidence.[23–28]

We recall that the cluster binding energies are with respect to energies of the isolated defects. The relatively high values for the binding energies may indicate that the isolated oxygen interstitial energy is unfavorable in the pure material; this is consistent with the fact that compositions greater than $x=7$ for undoped $YBa_2Cu_3O_x$ are not easy to attain. Our results emphasize the importance of the Coulomb term, together with lattice relaxation, as the driving force for the formation of interstitial oxygen, provided the necessary dopant aggregation occurs. Alternatively we see that the presence of trivalent impurities encourages interstitial site occupancy.

Of the tetramer geometries examined the high symmetry square configuration is found to be the most energetically favorable, with very similar stability for the dimer. Further enhancement of the binding energy occurs with the edge-shared hexamer which has a slightly larger value than for either the simple dimer or tetramer. Aggregation is, therefore, thermodynamically favored by a process that retains the basic square tetramer unit but increases the total number of dopant ions in the phase.

TABLE III. Calculated energetics of clusters of Fe^{3+} and oxygen interstitials on the Cu(1) layer.

Cluster	Total defect energy (eV)	Binding energy[a] (eV/dopant)
$(2Fe_{Cu}^{\cdot}\text{-}O_i'')$ dimer	−61.77	−2.91
$(4Fe_{Cu}^{\cdot}\text{-}2O_i'')$ tetramer		
Collinear	−122.14	−2.57
Square	−123.49	−2.90
Zigzag	−120.27	−2.10
$(6Fe_{Cu}^{\cdot}\text{-}4O_i'')$ hexamer	−206.33	−3.19
$(7Fe_{Cu}^{\cdot}\text{-}4O_i'')$ double chain	−226.69	−3.03

[a]Negative value indicates system is bound.

TABLE IV. Calculated energetics of clusters of Al^{3+} and oxygen interstitials on the Cu(1) layer.

Cluster	Total defect energy (eV)	Binding energy (eV/dopant)
$(2Al_{Cu}^{\cdot}\text{-}O_i'')$ dimer	−72.46	−2.74
$(4Al_{Cu}^{\cdot}\text{-}2O_i'')$ tetramer		
Collinear	−142.95	−2.25
Square	−144.83	−2.72
Zigzag	−142.34	−2.10
$(6Al_{Cu}^{\cdot}\text{-}4O_i'')$ hexamer	−237.40	−2.84
$(7Al_{Cu}^{\cdot}\text{-}4O_i'')$ double chain	−263.76	−2.80

However, it is not certain whether cluster growth by this mode of "edge sharing" would be limited, as is found in nonstoichiometric $Fe_{1-x}O$.[30] The alternative "corner sharing" of tetramer units leads to the double-chain configuration shown in Fig. 3, which is also calculated to have enhanced stability. This result is consistent with the interpretation of EXAFS data by Bridges *et al.*[25] who support the formation of chains of Fe (or Co) along the ⟨110⟩ direction. In either case, the increase in magnitude of the calculated binding energy as the size of the cluster increases provides evidence for the continuation of the aggregation process to yield larger clusters.

Note that clustering does not necessarily preclude the presence of isolated substitutionals, since cluster species will be in equilibrium with single defects as well as other cluster types. A difficulty encountered in these calculations is the additional, but uncertain, mode of rearrangement of the O(1) chain oxygen atoms on to the O(5) unoccupied sites, which may effect the stabilization of certain types of cluster. This is currently under investigation.

The general picture that emerges from our results is that dopants will associate to form clusters with substantial short-range order, and may act as important precursors to a final ordered phase. Below the phase transition concentration of dopants these well-defined clusters or microdomains coexist with predominantly undoped orthorhombic CuO structure in the basal plane. Further aggregation or ordering may, at a critical dopant concentration, result in the macroscopic structural change to tetragonal symmetry, although the crystal may contain orthorhombic regions on a microscopic level. As suggested by Jorgensen,[55] this has important implications with regard to whether $YBa_2Cu_3O_{7-x}$ must have orthorhombic symmetry, at least on a local scale, to exhibit superconductivity. Nevertheless, such defect clustering could play a major role in stabilizing the observed tetragonal structure.

Now focusing on the local dopant environment: an individual Fe (or Al) ion could, in principle have at least there site geometries with oxygen, namely, fourfold (square planer or pseudotetrahedral), fivefold (square pyramidal), or sixfold (octahedral) coordination. Within the clusters the dopant ions tend to have higher coordination than they would if they were isolated. Our results, therefore, suggest that the oxygen coordination number of Fe and Al will increase with increasing dopant content. From analysis of the various cluster configurations (shown in Figs. 1–3) we predict the predominance of fivefold pyramidal coordination with some sixfold coordination, which is consistent with recent XANES measurements of Fe- and Co-doped samples.[26,27]

C. Ion displacements

In addition to the calculation of binding energies, the simulation codes generate valuable information on the final atomic positions following lattice relaxation. The vector displacements of ions near the simple dimer configuration $(2M_{Cu}^{\cdot}\text{-}O_i'')$ as well as the calculated bond lengths are shown in Fig. 4. In Table V the relaxed positions and mean displacements of selected ions for the double-chain model are summarized.

Examination of these results reveal a substantial movement of lattice ions associated with dopant incorporation, thus inducing a significant perturbation in the local structure. In particular, we find large off-center displacement of the Fe^{3+} and Al^{3+} ions of 0.15 and 0.27 Å, respectively. Both dopants shift generally in the ⟨110⟩ direction leading to a noncentrosymmetric coordination. This is in agreement with EXAFS data,[25] which suggest an off-center model with a distorted Fe environment, and with neutron diffraction data[24] which show that Fe principally occupies a site displaced $(y, y, 0)$ from the Cu(1) (0, 0, 0) site where $y \sim 0.025$. Such displacements, together with the various possible Fe coordinations, could explain the observed data from ^{57}Fe Mössbauer measurements.

The atomic displacements found from both simulation and experiment may be expected partly on the basis of ion-size factors due to the difference in ionic radii between the dopant and host Cu^{2+} ions. Previous studies[56] have discussed off-center displacement in terms of the balance between overlap and polarization terms in the lattice energy. Since both Fe^{3+} and Al^{3+} are smaller than Cu^{2+} the overlap forces are reduced and, therefore, not great enough to oppose the movement of the substitutional ion off the normal chain site, with the resulting displacement stabilized by the lattice polarization energy. The successful prediction of this subtle effect thus provides further confirmation of the validity of the interatomic potentials used.

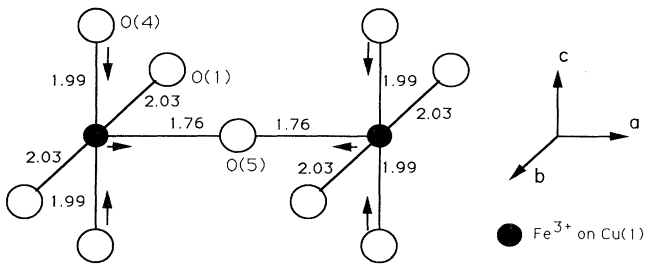

FIG. 4. Ion displacements and calculated bond lengths (in Å) for the Fe dimer configuration.

TABLE V. Relaxed positions and mean displacements of ions in the double-chain cluster.

Ion	Normal lattice site[a]	Final relaxed position	Displacement (Å)
M^{3+}	(0 0 0)	(0.04 0.01 0)Fe	0.15
		(0.07 0.01 0)Al	0.27
O(1)	(0 0.51 0)	(−0.10 0.50 0)Fe	0.37
		(−0.04 0.47 0)Al	0.21
O(4)	(0 0 0.48)	(−0.02 0 0.51)Fe	0.13
		(−0.02 0 0.49)Al	0.08
O(5)[b]	(0.5 0 0)	(0.5 −0.03 0)Fe	0.13
		(0.5 −0.08 0)Al	0.31

[a]Atomic coordinates in lattice units (a_0).
[b]Normally unoccupied in $YBa_2Cu_3O_7$.

Further analysis finds the neighboring O(4) apex ions drawing closer to the dopant sites by ~0.1 Å, and displacements as large as 0.4 Å for the O(1) chain ions in the *a* direction. Such movement of ions will obviously result in significant changes in local bond lengths. In Fig. 5 the final positions and calculated bond lengths are shown for the double-chain cluster, indicating Fe—O(1) bond lengths of ~2.01 Å and Fe—O(5) bond lengths of ~1.78 Å. There has been some conflicting information from diffraction and absorption studies in relation to local bond lengths. Yang *et al.*[27] find a similarity of Fe—O bond lengths (1.84 and 1.95 Å) with Co—O bond lengths (1.85 and 1.95 Å); whereas Bridges *et al.*[25] support the formation of zigzag chains with distinct long and short Fe—O bonds of 1.88 and 2.36 Å. Such discrepancies could be accounted for by different sample preparation, but also by the simultaneous presence of various cluster types with different geometries within the crystal lattice.

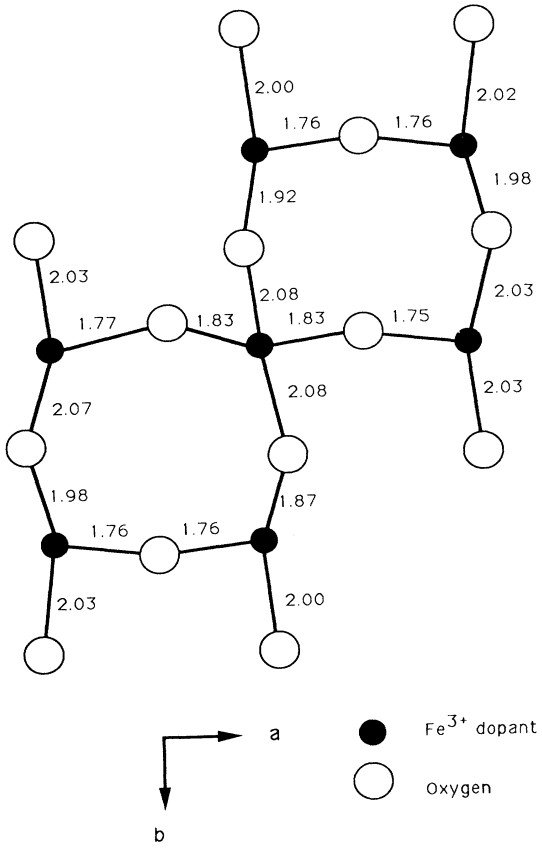

FIG. 5. Final relaxed positions and calculated bond lengths (in Å) for the ($7Fe'_{Cu}$-$4O''_i$) double-chain cluster.

It is now believed that superconductivity in $YBa_2Cu_3O_7$ is linked to charge-transfer effects[55] between the conduction layer, consisting of the CuO_2 planes separated by yttrium ions, and the charge "reservoir" layer consisting of the CuO chains, apex oxygens, and barium ions. The structural distortions and accompanying changes in bond lengths on doping have the effect of changing the carrier concentration in the chain layer and altering the coupling between the Cu(1) and Cu(2) layers particularly through small movements of the O(4) apex atom. In fact, our calculated M—O(4) bond lengths, listed in Table VI, show a lengthening for both Fe and Al. In this context we note that our previous investigation of dopant substitution[38] found a trend between T_c and calculated Cu(1)—O(4) bond lengths for divalent impurities. Thus local structural disorder will probably play a critical role in modifying the electronic structure and hence change the superconducting behavior.

TABLE VI. Calculated mean *M*—O(4) bond lengths for the hexamer and double-chain clusters.

Bond	*r* (Å)	Δ^b (Å)
Cu(1)—O(4)[a]	1.874	—
Hexamer:		
Fe—O(4)	2.123	0.249
Al—O(4)	2.025	0.151
Double chain:		
Fe—O(4)	2.105	0.231
Al—O(4)	1.974	0.100

[a]Undoped crystal.
[b]Difference with undoped bond length.

A final point of interest is in relation to ion diffusion. Due to the high degree of cluster stability (i.e., large binding energies) the diffusion of the impurity ion will probably be slow and make little contribution to ionic conductivity. Therefore, diffusion via an oxygen vacancy mechanism[39] would dominate as in the undoped material. This idea of immobilizing defects by being bound within clusters is not unusual and has been proposed to account for the variation of oxygen diffusion in Sr-doped La_2CuO_4 (Ref. 57) and is also observed in highly doped fluorite-structured oxides (e.g., CeO_2).[58]

IV. SUMMARY

In general the present study demonstrates the importance of local structural features in $YBa_2Cu_3O_7$, which are difficult to probe by conventional experimental techniques. Simulation techniques based on effective interatomic potentials are thus extremely useful in examining defect clustering on an atomic level. Our discussion has drawn attention to four main features of Fe^{3+} and Al^{3+} substitution.

(1) The large binding energies clearly indicate that there is a strong tendency toward cluster formation on the Cu(1) basal plane, with the presence of trivalent impurities promoting the occupancy of the oxygen interstitial site. Therefore, the dopant ions and incoming oxygen tend to associate into distinct clusters rather than being randomly distributed over the crystal lattice.

This is in agreement with the available experimental data which find evidence for Co^{3+} and Fe^{3+} clustering. Since there is limited experimental information for Al-substituted $YBa_2Cu_3O_7$ our results in this case have a clear predictive value.

(2) Of the clusters considered the hexamer and double-chain configurations appear to be the most energetically favorable. Such clusters will be in equilibrium with single defects, as well as other cluster types. Further aggregation could play a stabilizing role in the observed transition to tetragonal symmetry. However, the average tetragonal structure does not preclude the coexistence of orthorhombic domains.

(3) The Fe^{3+} and Al^{3+} coordination with oxygen is predicted to increase on doping with the predominance of fivefold pyramidal coordination. This accords with the observed site coordinations from x-ray absorption measurements.

(4) Dopant substitution leads to notable local distortion with extensive movement of ions that provide stabilizing relaxation. In particular, we calculate significant off-center displacement of both Fe^{3+} and Al^{3+} and find a lengthening of the M^{3+}—O(4) bond. This may be indicative of charge-transfer effects between the Cu(1) and Cu(2) layers, the importance of which has been suggested previously. These findings are consistent with off-center models proposed from neutron and EXAFS data and are particularly encouraging as predictions of off-center behavior provide a strict test for the potentials used.

Finally, due to the strong binding energies we expect relatively slow diffusion of the impurity species. Further studies are planned to explore this topic and will extend the work to investigate other examples of aliovalent doping in $YBa_2Cu_3O_7$.

ACKNOWLEDGMENTS

We are grateful to the University of Surrey for support of this work. We also thank the University of London Computer Centre for the facilities on the Cray XMP supercomputer.

[1]G. Xiao, F. H. Streitz, A. Garvin, Y. W. Du, and C. L. Chien, Phys. Rev. B **35**, 8782 (1987).

[2]Y. Maeno, T. Tomita, M. Kyogoku, S. Awaji, Y. Aoki, K. Hosino, A. Minami, and T. Fujita, Nature (London) **328**, 512 (1987).

[3]T. Siegrist, L. F. Schneemeyer, J. V. Waszczak, N. P. Singh, R. L. Opila, B. Batlogg, L. W. Rupp, and D. W. Murphy, Phys. Rev. B **36**, 8365 (1987).

[4]J. M. Tarascon, P. Barboux, P. F. Miceli, L. H. Greene, G. W. Hull, M. Eibschutz, and S. A. Sunshine, Phys. Rev. B **37**, 7458 (1988).

[5]J. Jung, J. P. Frank, W. A. Miner, and M. A. -K. Mohammed, Phys. Rev. B **37**, 7510 (1988).

[6]E. Takayama-Muromahci, Y. Uchida, and K. Kato, Jpn. J. Appl. Phys. **26**, L2087 (1987).

[7]R. J. Cava, B. Batlogg, R. M. Fleming, S. A. Sunshine, A. Ramirez, E. A. Rietman, S. M. Zahurak, and R. B. van Dover, Phys. Rev. B **37**, 5912 (1988).

[8]P. F. Miceli, J. M. Tarascon, L. H. Greene, P. Barboux, F. J. Rotella, and J. D. Jorgensen, Phys. Rev. B **37**, 5932 (1988).

[9]K. Zhang, B. Dabrowski, C. U. Segrè, D.G. Hinks, I. K. Schuller, J. D. Jorgensen, and M. Slaski, J. Phys. C **20**, L935 (1987).

[10]S. Katano, S. Funahashi, T. Hatano, A. Matsushita, K. Nakamura, T. Matsumoto, and K. Ogawa, Jpn. J. Appl. Phys. **26**, L1046 (1987).

[11]C. U. Segrè, B. Dabrowski, D. G. Hinks, K. Zhang, J. D. Jorgensen, M. A. Beno, and I. K. Schuller, Nature (London) **329**, 227 (1987).

[12]J. F. Bringley, T. M. Chen, B. A. Averilll, K. M. Wong, and S. J. Poon, Phys. Rev. B **38**, 2432 (1988).

[13]B. Jayaram, S. K. Agarwal, C. V. N. Rao, and A. V. Narlikar, Phys. Rev. B **38**, 2903 (1988).

[14]H. J. Rosen, R. M. Macfarlane, E. M. Engler, V. Y. Lee, and R. D. Jacowitz, Phys. Rev. **38**, 2460 (1988).

[15]I. Nowik, M. Kowitt, I. Felner, and E. R. Bauminger, Phys. Rev. B **38**, 6677 (1988).

[16]P. Zolliker, D. E. Cox, J. M. Tranquada, and G. Shirane, Phys. Rev. B **38**, 6575 (1988).

[17]M. F.Yan, W. W. Rhodes, and P. K. Gallagher, J. Appl. Phys. **63**, 821 (1988).

[18]Y. Xu, M. Suenaga, J. Tafto, R. L. Sabatini, A. R. Moodenbaugh, and P. Zolliker, Phys. Rev. B **39**, 6667 (1989).

[19]C. Blue, K. Elgaid, I. Zitkovsky, P. Boolchand, D. McDaniel, W. C. H. Joiner, J. Oostens, and W. Huff, Phys. Rev. B **37**, 5905 (1988).

[20]T. J. Kistenmacher, Phys. Rev. B **38**, 8862 (1988).
[21]C. Greaves and P. R. Slater, Physica C **161**, 245 (1989).
[22]F. Bridges, J. B. Boyce, T. Claeson, T. H. Geballe, and J. M. Tarascon, Phys. Rev. B **42**, 2137 (1990).
[23]P. Bordet, J. L. Hodeau, P. Strobel, M. Marezio, and A. Santoro, Solid State Commun. **66**, 435 (1988).
[24]B. D. Dunlap, J. D. Jorgensen, C. U. Segrè, A. E. Dwight, J. L. Matykiewicz, H. Lee, W. Peng, and C. W. Kimball, Physica C **158**, 397 (1989).
[25]F. Bridges, J. B. Boyce, T. Claeson, T. H. Geballe, and J. M. Tarascon, Phys. Rev. B **39**, 11 603 (1989).
[26]C. Y. Yang, S. M. Heald, J. M. Tranquada, Y. Xu, Y. L. Wang, A. R. Moodenbaugh, D. O. Welch, M. Suenaga, Phys. Rev. B **39**, 6681 (1989).
[27]C. Y. Yang, A. R. Moodenbaugh, Y. L. Wang, Y. Xu, S. M. Heald, D. O. Welch, M. Suenaga, D. A. Fischer, and J. E. Penner-Hahn, Phys. Rev. B **42**, 2231 (1990).
[28]S. Katsuyama, Y. Ueda, and K. Kosuge, Physica C **165**, 404 (1990).
[29]A. M. Stoneham and L. W. Smith, J. Phys. Condens. Matter **3**, 225 (1991).
[30]S. M. Tomlinson, C. R. A.Catlow, and J. H. Harding, J. Phys. Chem. Solids **51**, 477 (1990).
[31]V. Butler, C. R. A. Catlow, B. E. F. Fender, and J. H. Harding, Solid State Ionics **8**, 109 (1983).
[32]M. S. Islam and C. R. A. Catlow, J. Solid State Chem. **77**, 180 (1988).
[33]J. Corish, C. R. A. Catlow, P. W. M. Jacobs, and S. H. Ong, Phys. Rev. B **25**, 10 (1982); **25**, 6425 (1982).
[34]M. S. Islam, M. Leslie, S. M. Tomlinson, and C. R. A. Catlow, J. Phys. C **21**, L109 (1988).
[35]C. R. A. Catlow, S. M. Tomlinson, M. S. Islam, and M. Leslie, J. Phys. C. **21**, L1085 (1988); X. Zhang and C. R. A. Catlow, Physica C **173**, 25 (1991).
[36]N. L. Allan and W. C. Mackrodt, Philos. Mag. A **58**, 555 (1988).
[37]R. C. Baetzold, Phys. Rev. B **38**, 11 304 (1988); **42**, 56 (1990).
[38]M. S. Islam and R. C. Baetzold, Phys. Rev. B **40**, 10 926 (1989).
[39]M. S. Islam, Supercond. Sci. Technol. **3**, 531 (1990).
[40]W. C. Mackrodt, Supercond. Sci. Technol. **1**, 343 (1989).
[41]M. Leslie, Solid State Ionics **8**, 243 (1983).
[42]M. J. Norgett (unpublished).
[43]C. R. A. Catlow, in *Computer Simulation of Solids,* Vol. 166 of *Lecture Notes in Physics,* edited by C. R. A. Catlow and W. C. Mackrodt (Springer-Verlag, Berlin, 1982).
[44]C. R. A. Catlow, Annu. Rev. Mater. Sci. **16**, 517 (1986).
[45]A. M. Stoneham and J. H. Harding, Ann. Rev. Phys. Chem. **37**, 53 (1986).
[46]B. G. Dick and A. W. Overhauser, Phys. Rev. **112**, 90 (1958).
[47]S. Horn, J. Cai, S. A. Shaheen, Y. Jeon, M. Croft, C. L. Chang, and M. L. denBoer, Phys. Rev. B **36**, 3985 (1987).
[48]A. Fujimore, E. Takayami-Muromachi, and Y. Uchida, Solid State Commun. **63**, 857 (1987).
[49]T. Iwazumi, I. Nakai, M. Izumi, H. Oyanagi, H. Sawada, H. Ikeda, Y. Saito, Y. Abe, K. Takita, and R. Yoshizaki, Solid State Commun. **65**, 213 (1988).
[50]J. A. Yarmoff, D. R. Clarke, W. Drube, U. O. Karlsson, A. Taleb-Ibrahimi, and F. J. Himpsel, Phys. Rev. B **36**, 3967 (1987).
[51]G. V. Lewis and C. R. A. Catlow, J. Phys. C **18**, 1149 (1985).
[52]N. F. Mott and M. J. Littleton, Trans. Faraday Soc. **34**, 485 (1938).
[53]A. B. Lidiard, J. Chem. Soc. Faraday Trans. 2, **85**, 341 (1989).
[54]F. A. Kroger and H. J. Vink, Solid State Phys. **3**, 307 (1956).
[55]J. D. Jorgensen, Nature (London) **349**, 565 (1991).
[56]J. A. D. Matthew, Solid State Commun. **3**, 365 (1965).
[57]J. L. Routbort, S. J. Rothman, B. K. Flandermeyer, L. J. Nowicki, and J. E. Baker, J. Mater. Res. **3**, 116 (1988).
[58]R. Gerhardt-Anderson and A. S. Nowick, Solid State Ionics **5**, 547 (1981).